The response of high-impact blocking weather systems to climate change

AGU PUBLICATIONS

Geophysical Research Letters

RESEARCH LETTER
10.1002/2016GL069725

Key Points:
- Enhanced warming both in the tropics and over the Arctic act to reduce the frequency of blocking
- Tropical warming is more important in terms of the uncertainty in projected blocking changes
- The Arctic also affects the temperature anomalies experienced during blocking

Supporting Information:
- Supporting Information S1

Correspondence to:
T. Woollings,
Tim.Woollings@physics.ox.ac.uk

Citation:
Kennedy, D., T. Parker, T. Woollings, B. Harvey, and L. Shaffrey (2016), The response of high-impact blocking weather systems to climate change, *Geophys. Res. Lett.*, *43*, doi:10.1002/2016GL069725.

Received 24 MAR 2016
Accepted 20 JUN 2016
Accepted article online 27 JUN 2016

The response of high-impact blocking weather systems to climate change

Daniel Kennedy[1], Tess Parker[1], Tim Woollings[1], Benjamin Harvey[2], and Len Shaffrey[2]

[1] Atmospheric, Oceanic and Planetary Physics, Department of Physics, University of Oxford, Oxford, UK, [2]National Centre for Atmospheric Science, Department of Meteorology, University of Reading, Reading, UK

Abstract Midlatitude weather and climate are dominated by the jet streams and associated eastward moving storm systems. Occasionally, however, these are blocked by persistent anticyclonic regimes known as blocking. Climate models generally predict a small decline in blocking frequency under anthropogenic climate change. However, confidence in these predictions is undermined by, among other things, a lack of understanding of the physical mechanisms underlying the change. Here we analyze blocking (mostly in the Euro-Atlantic sector) in a set of sensitivity experiments to determine the effect of different parts of the surface global warming pattern. We also analyze projected changes in the impacts of blocking such as temperature extremes. The results show that enhanced warming both in the tropics and over the Arctic act to strengthen the projected decline in blocking. The tropical changes are more important for the uncertainty in projected blocking changes, though the Arctic also affects the temperature anomalies during blocking.

1. Introduction

The response of the atmospheric circulation to climate change is key to understanding changes on regional scales, such as the response of the jet streams and storm tracks. While there is some confidence in those aspects of climate change that are related to thermodynamics, such as global surface temperature, there is larger uncertainty around the atmospheric circulation response, which is controlled by dynamics [*Shepherd*, 2015]. In the extratropics, key dynamical components of the general circulation include the jet streams, storm tracks, and atmospheric blocking [*Woollings*, 2010]. The emerging understanding in current research suggests that changes in the large-scale temperature gradients of the atmosphere can be used to explain changes in the jets and storm tracks [e.g., *Harvey et al.*, 2013, 2015].

The weather and climate of the midlatitudes are dominated by the prevailing westerly winds and accompanying cyclonic storm systems. However, the westerly flow may be blocked or split and the cyclonic storm systems diverted by persistent quasi-stationary anticyclones known as blocks [*Rex*, 1950]. These blocking events often lead to damaging impacts such as dry, cold winters or wet conditions [*Sillmann and Croci-Maspoli*, 2009], and extremes of surface temperature through large-scale advection and radiative forcing [*Pfahl and Wernli*, 2012; *Masato et al.*, 2014]. For example, blocking was responsible for the very cold European winter of 2009/2010 [*Cattiaux et al.*, 2010] and the 2010 Russian heat wave [*Matsueda*, 2010; *Dole et al.*, 2011] and for steering Hurricane Sandy onto the coast of the United States of America [*Torn et al.*, 2012].

Projections of the response of atmospheric blocking to global warming indicate that while the duration of blocking remains fairly constant under different greenhouse gas (GHG) scenarios, the frequency of blocking demonstrates a robust reduction [*Matsueda et al.*, 2009; *Scaife et al.*, 2010; *Barnes et al.*, 2011; *Dunn-Sigouin and Son*, 2013]. However, climate models have relatively coarse resolution and do not accurately represent blocking in the current climate, largely as the result of biases in the model mean state [*Scaife et al.*, 2010; *Berckmans et al.*, 2013] such as biases in the tropospheric jet latitude [*Anstey et al.*, 2013; *Masato et al.*, 2013]. Furthermore, model performance differs over the Pacific and Euro-Atlantic sectors, with a negative bias in blocking frequency usually seen over Europe [*Matsueda*, 2009; *Masato et al.*, 2013, 2014].

Amplified Arctic warming is a key feature of the warming pattern. Some studies of the recent loss of Arctic sea ice have suggested that amplified Arctic warming might lead to an increase in the occurrence of blocking or related stationary weather patterns [e.g., *Liu et al.*, 2012; *Francis and Vavrus*, 2012; *Mori et al.*, 2014]. This is at

odds with the projected future decline of blocking, so one aim of this paper is to determine how the projected blocking changes are affected by the temperature changes in the Arctic and elsewhere.

The zonal-mean response to increased GHG concentrations is characterized by enhanced upper tropospheric warming in the tropics as well as surface warming near the poles in winter [e.g., *Harvey et al.*, 2015; *Barnes and Screen*, 2015], and these features may not be independent [*Deser et al.*, 2016]. The North Atlantic storm track may be influenced by local sea surface temperatures (SSTs) [*Wilson et al.*, 2009; *Brayshaw et al.*, 2011] as well as the distribution of Arctic sea ice concentration (SIC) [*Deser et al.*, 2000; *Magnusdottir et al.*, 2004]. *Harvey et al.* [2015] identified potential physical drivers of changes to the storm track and assessed their influence using a series of atmosphere-only general circulation model (GCM) experiments forced by perturbations in the SST and SIC fields. Their study suggests that the storm track response is driven by competing upper and lower tropospheric temperature gradients due to tropical and Arctic warming [*Held*, 1993; *Butler et al.*, 2010; *Harvey et al.*, 2013]. *Harvey et al.* [2015] also suggest that the tropics dominate in setting the patterns of change in the storm track but that the Arctic is the primary source of spread in the projections of storm track changes.

In the present study, the experiments of *Harvey et al.* [2015] are used to examine the changes in blocking as a result of factors such as enhanced Arctic warming or reduced North Atlantic warming. The main focus of this study is to investigate the underlying processes that control the projected changes in future blocking, as well as the uncertainty in these changes. A secondary investigation relates to the projected changes in the impacts of blocking, such as large-scale advection, and how these changes combine to result in changes in extremes of temperature.

The experimental design is described in section 2, and section 3 discusses the projected changes in blocking under the different scenarios. Section 4 examines the underlying processes which lead to changes in blocking, with an overview given in section 5. Section 6 looks at the impacts of blocking on temperature anomalies over Europe.

2. Data and Methodology

The original series of sensitivity experiments were performed by *Harvey et al.* [2015] using HadGAM1, the atmosphere component of the Hadley Centre's HadGEM1 GCM [*Johns et al.*, 2006; *Martin et al.*, 2006], at a grid point resolution of $1.875^\circ \times 1.25^\circ$ with 38 vertical layers between the surface and the model top at 39 km altitude. This model has a reasonable simulation of blocking in the present-day climate (see *Anstey et al.* [2013] or *Masato et al.* [2013] for analysis of a similar model version). Six of these experiments are used in the present study, which differ only in the prescribed SST, SIC, and well-mixed GHG fields. These potential physical drivers of storm track changes are independently perturbed by a range of values, the magnitude of which represents the spread of responses found in the Coupled Model Intercomparison Project phase 3 (CMIP3) models. The response of blocking to climate change in this model is in good agreement with other models in Coupled Model Intercomparison Project phase 5 (CMIP5) [*Masato et al.*, 2013; *Anstey et al.*, 2013] and also CMIP3 [*Barnes et al.*, 2011].

The first pair of experiments (designated "Control") consists of a present-day control run (CTRL) with fixed late twentieth century GHG values (1961–2000), CMIP3 multimodel mean 20C3M SSTs, and reconstructed 20C3M SIC, and a run (A1B) using projected late 21st century (2061–2100) fixed GHG values, CMIP3 mean SRESA1B SSTs, and reconstructed SRESA1B SIC. Two further pairs of perturbation runs are designed to isolate the different factors that may be responsible for changes in blocking. In the first pair of perturbed experiments ("Arctic"), designated the Arctic Warm (ARCW) or Arctic Cold (ARCC) experiments, the Arctic sea ice extent is retreated at each longitude by the distance retreated in the A1B experiment ± 1 standard deviation of the range of distances in the CMIP3 models (see Figures S3b and S3e in the supporting information). The SST field in the ice edge region of the A1B experiment is perturbed to provide a warmer or cooler ice edge region respectively as expected. The second pair of perturbed experiments ("Uniform"), in which a uniform SST anomaly of ± 0.87 K is applied to the global A1B SST field, are designated as the Uniform Warm (UFMW) or Uniform Cold (UFMC) experiments, respectively. The magnitude of this perturbation is 3 times the standard deviation of the tropical (i.e., latitudes within 30° of the equator) SST responses in the CMIP3 models, as this was found to give spread in the 250 hPa temperature gradients which is equivalent to one standard deviation of the spread across the CMIP3 multimodel ensemble (see Figures S1c and S1f in the supporting information). The Uniform experiments use the reconstructed SRESA1B SIC field. Experiments were performed for 60 years

for the CTL and A1B experiments and 40 years for each of the other four experiments. See *Harvey et al.* [2015], Figures S1–S3 and Table S1 in the supporting information for full details of the experimental design.

A number of definitions of and indices for identifying blocking exist, some focused on the anticyclonic nature of blocking via reversals of the meridional geopotential height gradient [e.g., *Tibaldi and Molteni*, 1990] and others focused on the dynamical Rossby wave breaking interpretation of blocking as diagnosed by reversals of the meridional gradient of potential temperatures on the dynamical tropopause [*Pelly and Hoskins*, 2003]. The blocking detection method used in the present study is the two-dimensional extension of the *Tibaldi and Molteni* [1990] method introduced by *Scherrer et al.* [2005]. The blocking index is calculated based on 500 hPa geopotential height gradients at central grid latitudes between 35° and 75°N (in 2.5° steps), with a distance of 15° between the central latitude ϕ_0 and the northern and southern latitudes, ϕ_N and ϕ_S, respectively. The northern G_N and southern G_S gradients are then calculated as

$$G_N = \frac{z_{500}(\phi_N) - z_{500}(\phi_0)}{\phi_N - \phi_0}, \qquad G_S = \frac{z_{500}(\phi_0) - z_{500}(\phi_S)}{\phi_0 - \phi_S} \tag{1}$$

where z_{500} is the 500 hPa geopotential height.

A geopotential height gradient threshold of >0 and <-10 m per degree latitude for G_S and for G_N, respectively, together with a 5 day persistence criterion are enforced at every grid point. This method identifies blocks that are stationary in space and uninterrupted in time, characteristics typical of mature blocking events. This index gives a climatology of blocking with maxima over the North Pacific, Greenland and the North Sea [see *Scherrer et al.*, 2005].

In this study, the blocking index is calculated from the daily mean geopotential height data for each experiment. The change in the blocking index is then calculated for each pair of runs, viz., A1B minus CTRL, ARCW minus ARCC, and UFMW minus UFMC. Statistical significance is calculated at each grid point using a two-tailed Student's *t* test with a significance level of 95% to identify regions where the changes in blocking are significant.

3. Projected Changes in Blocking

In order to isolate the potential causes of projected changes in blocking frequency, the blocking index is calculated for each experiment and the differences in frequency between each pair of experiments is derived for both winter (December-January-February, DJF) and summer (June-July-August, JJA) (Figure 1). Note that this model has a reasonable simulation of blocking in the present-day climate, with frequencies of 0.03 days^{-1} over Greenland and the North Sea [cf. *Anstey et al.*, 2013, Figure 1].

For the Control pair of experiments, in DJF there is a reduction in blocking frequency under the A1B scenario in both the high- and low-latitude north Atlantic (Figure 1a), with statistically significant changes over Greenland and over the oceans to the west of Scandinavia and southwestern Europe. This result is similar to many other models [*Masato et al.*, 2013] and is consistent with reduced north-south wobbling and increased pulsing (i.e., variations in jet speed) of the North Atlantic jet in the CMIP5 models with increased GHGs demonstrated by *Barnes and Polvani* [2013], since the variability of the eddy-driven jet is strongly tied to blocking frequency [*Woollings et al.*, 2008; *Davini et al.*, 2012]. For JJA, the response in the Euro-Atlantic sector is small (Figure 1d).

In winter, there is a general reduction in blocking associated with a warmer Arctic (Figure 1b). The exception is an increase in blocking frequency over northern Scandinavia, although this change is not statistically significant. This result is opposite to the hypothesis of *Francis and Vavrus* [2012], who suggested that more persistent weather patterns might be occurring due to recently observed Arctic amplification, but in agreement with the findings of *Hassanzadeh et al.* [2014] who concluded that decreases in the midlatitude to pole near-surface temperature gradient produces a robust decrease in blocks. In summer, there is also no clear pattern of increase, with a mixture of increased and decreased blocking frequency and few statistically significant points (Figure 1e). This is perhaps not surprising given the small response of the mean state to SIC changes in summer (Figures 2e, S1e, S2e, and S3e).

Uniform warming shows a general decrease in blocking frequency in DJF (Figure 1c), with large areas of statistical significance over the Euro-Atlantic sector where the pattern is in qualitative agreement with that of the A1B warming scenario (Figure 1a). This result is in agreement with *Harvey et al.* [2015], who found similar

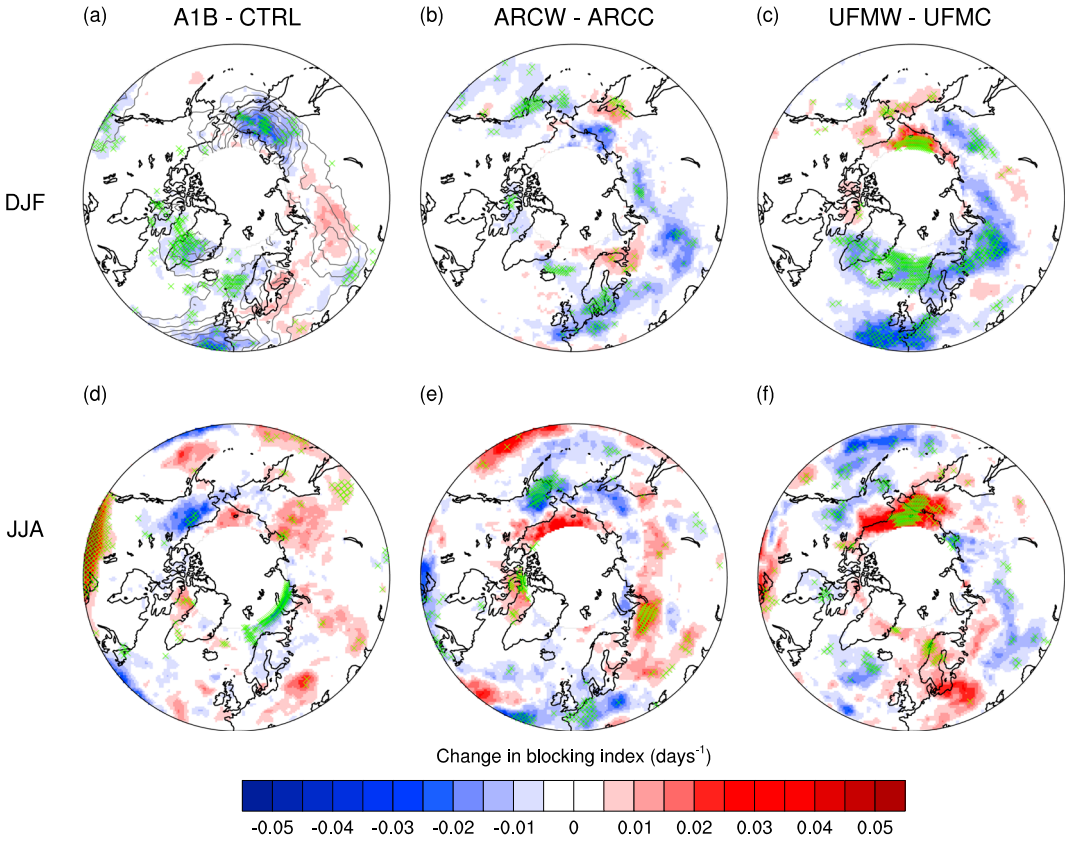

Figure 1. The changes in the blocking index (days^{-1}) between the pairs of climate change experiments. The change for (top row) DJF and (bottom row) for JJA for the (a and d) Control, (b and e) Arctic, and (c and f) Uniform pairs of simulations. Green crosses indicate areas where the change is statistically significant at the 95% level. The grey contours in Figure 1a show the climatology for the CTRL experiment.

changes in the storm tracks under A1B warming. The changes under uniform warming over Europe are almost in quadrature with those under Arctic warming (Figure 1b). In JJA there are weak increases in blocking over eastern Europe and decreases over western Europe (Figure 1f).

4. Underlying Processes Leading to Changes in Blocking

4.1. Changes in Upper Level Westerly Flow

Changes in the meridional temperature gradient under the various climate change scenarios will give rise to changes in the prevailing westerly winds. Figure 2 shows the changes in the zonal component of the wind at 250 hPa for the three pairs of experiments. In winter (DJF), stronger westerlies in the Euro-Atlantic sector may result in reduced blocking in this region, as the stronger jet extends further eastward and blocking occurs further downstream [*Barnes and Polvani*, 2013; *de Vries et al.*, 2013]. This is seen in the A1B and UFMW experiments (Figures 2a and 2c). Under Arctic warming, the westerlies are weaker at higher latitudes over Europe (Figure 2b). As a result, the second condition for the identification of blocking ($G_N < -10$ m) becomes more difficult to satisfy, leading to a reduction in the frequency of blocking. The wind responses over the Euro-Atlantic region in the ARCW and UFMW experiments are very different, and the spatial patterns are in quadrature; however, the ARCW response is at higher latitudes, and thus, a reduction in blocking is possible in both cases [cf. *Harvey et al.*, 2015; *Deser et al.*, 2000]. These differences in the wind responses emphasize the fact that the details of the wind changes are important when assessing changes in blocking, and not just the sign of the change in the westerly winds.

A link to the changes in the westerly winds is also evident in summer; for example, in the UFMW experiment in JJA the jet shifts poleward, leading to weaker winds over central Europe and thus an increase in blocking frequency in that region (Figure 2f).

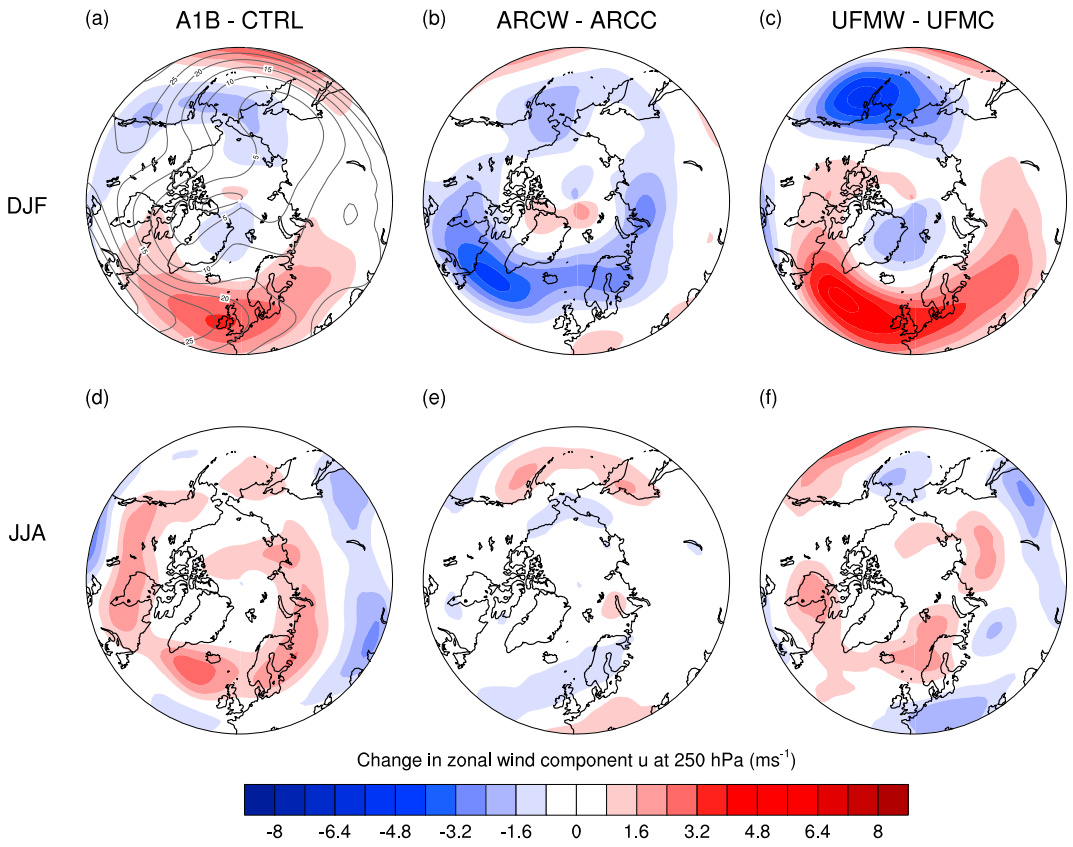

Figure 2. As for Figure 1 but for the changes in the 250 hPa westerly wind component (ms^{-1}).

4.2. Changes in the Mean State

Section 4.1 showed that the changes in the mean westerly winds are consistent with the changes in blocking. It is of interest to test whether the blocking changes may be explained by the changes in the mean state, at least in a statistical sense, or whether changes in some additional factor such as storm track variance are required [*Hassanzadeh and Kuang*, 2015]. Naturally, the mean state itself may be influenced by the changes in blocking; however, much more data would be required to detect changes in the shape of the distribution [cf. *de Vries et al.*, 2013]. In this study, a synthetic data test was created by adding the 500 hPa geopotential height (z_{500}) field from the "cold" simulation in each pair of experiments to the difference in the mean z_{500} fields between the "warm" and "cold" simulations. The blocking index is then calculated as before on this synthetic data set. The results (not shown) reveal similar spatial patterns of blocking to those found in the real data and which were discussed in section 3. Statistical significance testing (as defined in section 2) confirms that the changes in blocking frequency seen in the simulations above are well described by the mean state change (i.e., the difference between the real and synthetic data is not significant).

5. Overview of Changes in Blocking

The changes to future blocking in summer (JJA) are generally noisy, with little statistical significance, and there is no clear decrease in blocking frequency as is seen in winter (DJF) (Figure 1) [cf. *Masato et al.*, 2013]. If summer blocking frequency does not decrease in line with the decreases seen in winter, this will have implications for heat waves in the future. The response of blocking in UFMW (Figure 1f) is stronger, and covers a greater area, than the response to ARCW (Figure 1e). Although both warmings contribute to the spread in the response, the uniform warming is more important. This is to be expected, due to the link between atmospheric blocking and upper level Rossby wave breaking. An unexpected result is that the ARCW, as well as the UFMW, experiment results in reduced blocking frequency, although the reductions are in slightly different places in the two experiments. This can be understood by the changes in the mean state and the effect of changes in the jet on the preferred blocking regions.

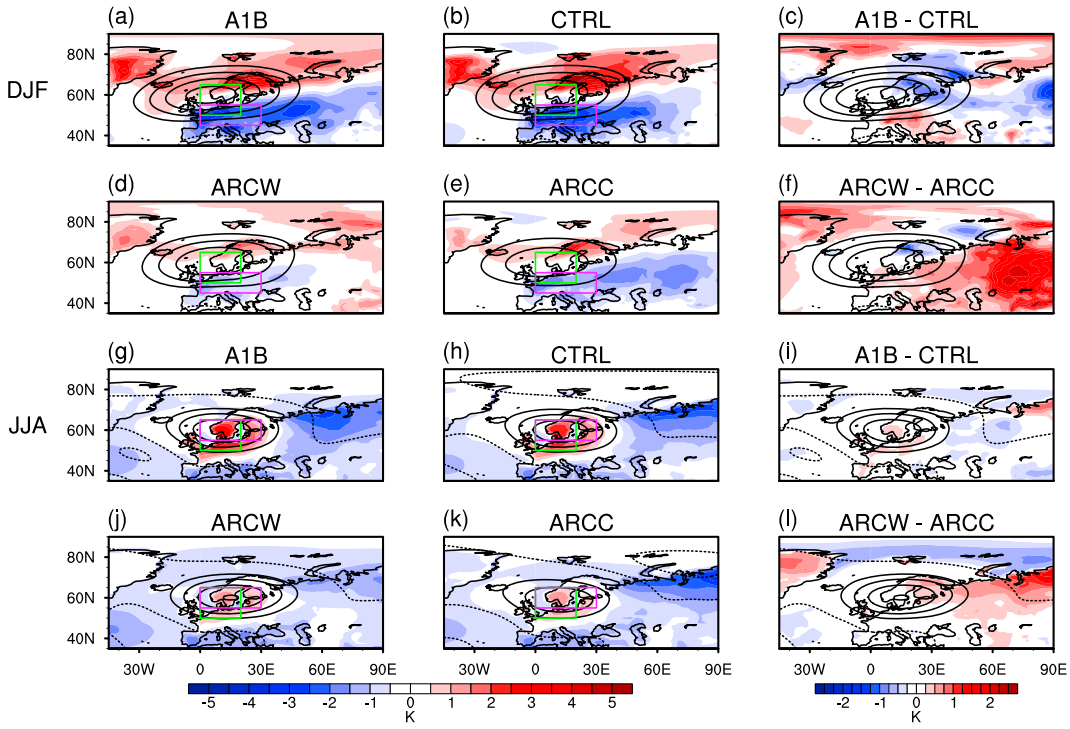

Figure 3. Surface temperature anomalies (color shading) and z_{500} anomalies (contoured at 50 m intervals for DJF, 25 m intervals for JJA, with zero contour omitted) during European blocks in the region from (0–20°E, 50–65°N) (green box) during (a–f) DJF and (g–l) JJA. The z_{500} anomalies in Figures 3c and 3i are those for the A1B and in Figures 3f and 3l for the ARCW experiments, respectively. The pink boxes denote the areas over which the temperature distributions in Figure 4 are taken. Note that the widespread cold anomalies in JJA are a consequence of the intraseasonal variation, with blocking more frequent in early summer.

6. Impacts of Blocking-Temperature Anomalies

One of the important consequences of projected changes in blocking is the resulting changes in temperature, particularly in temperature extremes such as cold outbreaks or heat waves. In order to determine the impacts of changes in blocking on temperature anomalies over Europe, a box from 0–20°E, 50–65°N is chosen as the test region (see green boxes in Figure 3). The purpose of this example is to illustrate the impacts of blocking on one particular region. For days on which a block has been identified in the test region, the anomalies from the climatology for each experiment are calculated for surface temperature and z_{500} (Figure 3).

For winter days (DJF) on which a blocking event is identified in the box, the warm anomalies at high latitudes are more widely spread over the Arctic in the A1B simulation (Figure 3a) than in the CTRL (Figure 3b), in agreement with *Masato et al.* [2013] (Figure 3c). Over Europe, the temperature anomalies associated with blocking weaken in the A1B experiment, with temperatures slightly warmer over central Europe and cooler over Scandinavia (Figure 3c). These changes are consistent with the expected changes in large-scale thermal advection [*Holmes et al.*, 2015], as the easterly winds to the south of the anticyclone are warmed by the continental warming and the westerly winds to the north are cooled due to the Atlantic minimum in warming. For the Arctic pair of experiments, it is clear that a warmer Arctic limits the extent of cold temperatures into Asia (Figures 3d–3f) as the northerly winds associated with the block are warmer in the ARCW than in the ARCC simulation. This is in contrast to the results of *Mori et al.* [2014], in a study based on a regional decline in sea ice in the Barents-Kara Sea, who found an increase in blocking between 0 and 90°E and an increase in the probability of severe winters in central Eurasia. It is not clear whether this discrepancy arises from differences in the pattern of forcing or the model and analysis methods used. There is not much impact on western Europe, as the northerly wind anomalies are further to the east. For blocks located further west, e.g., for Atlantic blocking, the warm anomalies would presumably extend into western Europe also [*Masato et al.*, 2013]. In JJA (Figures 3g–3l) the temperature differences are smaller, though again the cold anomalies underlying northerly winds weaken in the ARCW experiment (Figure 3l).

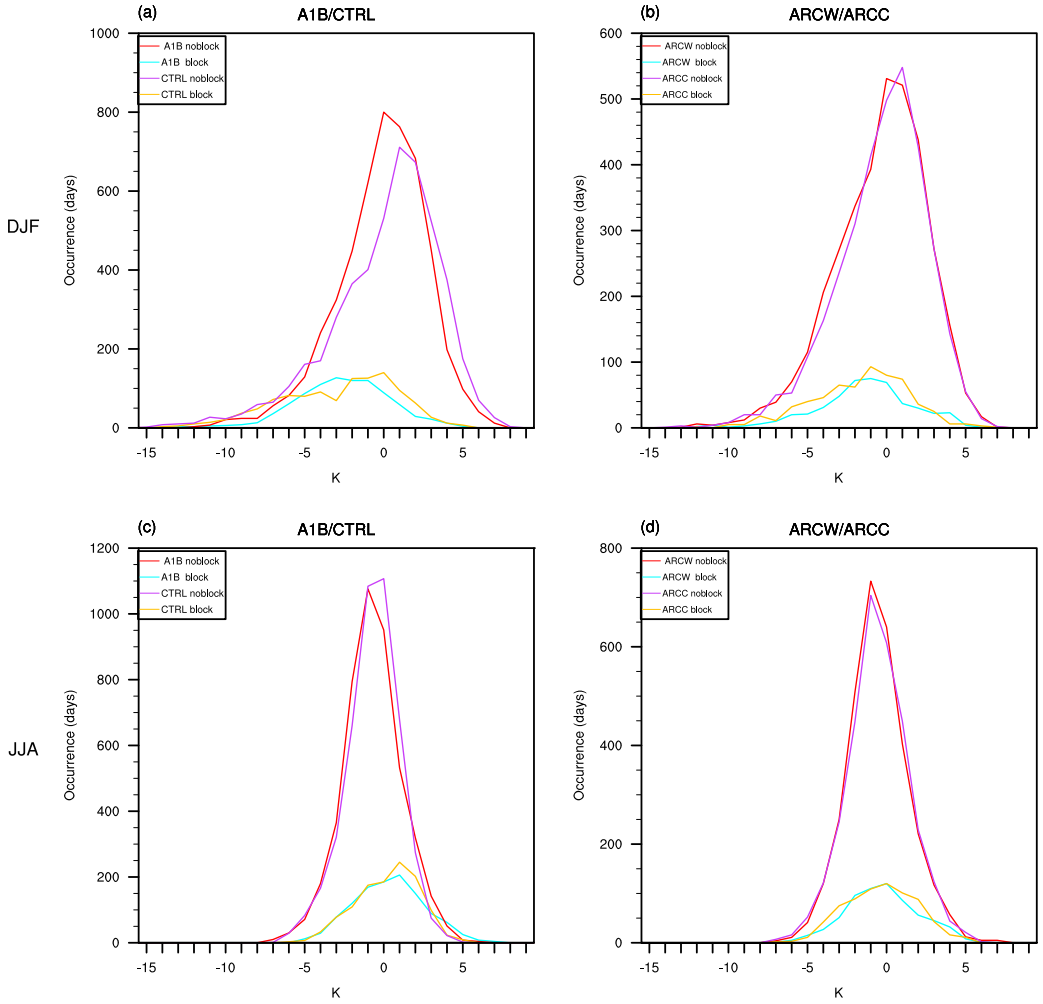

Figure 4. Surface temperature anomaly distributions during European blocks in the region from (0–20°E, 50–65°N) (as indicated by the green boxes in Figure 3) for the (a and c) Control and (b and d) Arctic pair of experiments. Figures 4a and 4b show results for DJF, taken over the region from (0–30°E, 45–55°N) and Figures 4c and 4d for JJA, taken over the region from (0–30°E, 55–65°N) (as indicated by the pink boxes in Figure 3).

In order to examine changes in the distribution of temperatures both during blocking events and when blocking is not present, temperature anomalies are calculated for two areas of interest: 0–30°E, 45–55°N in winter and 0–30°E, 55–65°N in summer (see pink boxes in Figure 3). The probability distributions of these anomalies, which again are anomalies from the climatology for each experiment, are shown in Figure 4. The local occurrence of blocking accounts for some of the coldest anomalies in both the Control and Arctic experiments. Note that some of the very cold no-blocking days may feature blocking outside of the chosen region, for example, over Greenland, which would correspond to a negative NAO event. The distribution of temperature anomalies in the A1B experiment is narrowed relative to CTRL for both blocked and nonblocked days (Figures 4a and 4c). This is likely due to the changes in thermal advection resulting from weakened horizontal temperature gradients [*Holmes et al.*, 2015]. The reduction in the number of blocking days is also apparent, and hence, both of these effects contribute to a reduction in the number of extreme cold days (e.g., anomalies <−5 K). These changes in temperature anomalies are of course superimposed on a considerable mean warming.

7. Conclusions

This study has investigated how the spatial distribution and impact of atmospheric blocking is influenced by different components of the global warming pattern. There is a focus on wintertime and on the Euro-Atlantic sector, but results were presented hemispherically and for summer for completeness. Simulations were analyzed from an atmospheric model forced to recreate the spread in upper and lower level temperature gradient

changes which result from tropical and Arctic warming, respectively. This showed that spread in the tropical response, and hence the upper level temperature gradient, has a greater effect on uncertainty in projected blocking changes than the Arctic response does. This is perhaps to be expected given the close connection between blocking and upper level Rossby wave breaking.

One unexpected result is that the response to Arctic warming is a decrease in blocking over Eurasia, which contrasts with expectations based on thermal wind balance. Hence, enhanced warming over both the tropics and the pole leads to reductions in blocking, although the precise location of these reductions differs. This can be understood from the structure in the zonal wind response and how this aligns with the blocking regions. The changes in blocking have been found to be consistent with the mean state response to forcing, so it is likely (but not guaranteed) that they occur as a consequence of the mean state response. An important caveat is that only one climate model and a single blocking index are used here. It would be interesting to repeat these experiments with different models, especially since many models show little to no relationship between Arctic warming and midlatitude blocking [*Woollings et al.*, 2015; *Barnes and Polvani*, 2015].

While Arctic warming was found to be of secondary importance for changes in blocking occurrence, it does have a clear effect on the impacts of blocking. These were assessed by considering the anomalies in surface temperature experienced during blocking. Focusing on winter, this showed that a stronger Arctic warming restricts the region of cold anomalies during European blocking, which would otherwise extend much deeper into Asia.

Changes in the temperature anomalies during blocking are generally consistent with the expectations from changes in thermal advection resulting from altered horizontal temperature gradients. For example, the cold anomalies over central Europe during winter blocking are weakened in the A1B experiment as the easterly winds bring air from continental regions which have warmed strongly. A reduction in extreme cold anomalies arises from this effect in combination with a reduction in the occurrence of blocking.

Acknowledgments
This work was supported in part by the Natural Environment Research Council project Improving Predictions of Drought for User Decision-Making (IMPETUS, NE/L01047X/1). D.K. was supported by the UK Met Office Academic Partnership. The model data used in this study are available from the authors on request. The authors wish to thank two anonymous reviewers for their helpful comments.

References

Anstey, J. A., P. Davini, L. J. Gray, T. J. Woollings, N. Butchart, C. Cagnazzo, B. Christiansen, S. C. Hardiman, S. M. Osprey, and S. Yang (2013), Multi-model analysis of Northern Hemisphere winter blocking. Part II: Future projections, *J. Geophys. Res. Atmos.*, *118*, 3956–3971, doi:10.1002/jgrd.50231.

Barnes, E. A., and L. Polvani (2013), Response of the midlatitude jets, and of their variability, to increased greenhouse gases in the CMIP5 models, *J. Clim.*, *26*, 7117–7135, doi:10.1175/CLDI-D-12-00536.1.

Barnes, E. A., and L. M. Polvani (2015), CMIP5 projections of Arctic amplification, of the North American/North Atlantic circulation, and of their relationship, *J. Clim.*, *28*, 5254–5271, doi:10.1175/JCLI-D-14-00589.1.

Barnes, E. A., and J. A. Screen (2015), The impact of Arctic warming on the midlatitude jet-stream: Can it? Has it? Will it?, *WIREs Clim. Change*, *6*, 277–286, doi:10.1002/wcc.337.

Barnes, E. A., J. Slingo, and T. Woollings (2011), A methodology for the comparison of blocking climatologies across indices, models and climate scenarios, *Clim. Dyn.*, *38*, 2467–2481, doi:10.1007/s00382-011-1243-6.

Berckmans, J., T. Woollings, M. E. Demory, P. L. Vidale, and M. Roberts (2013), Atmospheric blocking in a high resolution climate model: Influences of mean state, orography and eddy forcing, *Atmos. Sci. Lett.*, *14*(1), 34–40, doi:10.1002/asl2.412.

Brayshaw, D. J., B. Hoskins, and M. Blackburn (2011), The basic ingredients of the North Atlantic storm track. Part II: Sea surface temperatures, *J. Atmos. Sci.*, *68*, 1784–1805, doi:10.1175/2011JAS3674.1.

Butler, A. H., D. W. J. Thompson, and R. Heikes (2010), The steady-state atmospheric circulation response to climate change-like thermal forcings in a simple general circulation model, *J. Clim.*, *23*, 3474–3496, doi:10.1175/2010JCLI3228.1.

Cattiaux, J., R. Vautard, C. Cassou, P. Yiou, V. Masson-Delmotte, and F. Codron (2010), Winter 2010 in Europe: A cold extreme in a warming climate, *Geophys. Res. Lett.*, *37*, L20794, doi:10.1029/2010GL044613.

Davini, P., C. Cagnazzo, R. Neale, and J. Tribbia (2012), Coupling between Greenland blocking and the North Atlantic Oscillation pattern, *Geophys. Res. Lett.*, *39*, L14701, doi:10.1029/2012GL052315.

Deser, C., J. E. Walsh, and M. Timlin (2000), Arctic sea ice variability in the context of recent atmospheric circulation trends, *J. Clim*, *13*, 617–633, doi:10.1175/1520-0442(2000)013<0617:ASIVIT>2.0.CO;2.

Deser, C., L. Sun, R. A. Tomas, and J. Screen (2016), Does ocean coupling matter for the northern extra-tropical response to projected Arctic sea ice loss?, *Geophys. Res. Lett.*, *43*, 2149–2157, doi:10.1002/2016GL067792.

de Vries, H., T. Woollings, J. Anstey, R. J. Haarsma, and W. Hazeleger (2013), Atmospheric blocking and its relation to jet changes in future climate, *Clim. Dyn.*, *41*, 2643–2654, doi:10.1007/s00382-013-1699-7.

Dole, R., M. Hoerling, J. Perlwitz, J. Eischeid, P. Pegion, T. Zhang, X.-W. Quan, T. Xu, and D. Murray (2011), Was there a basis for anticipating the 2010 Russian heat wave?, *Geophys. Res. Lett.*, *38*, L06702, doi:10.1029/2010GL046582.

Dunn-Sigouin, E., and S.-W. Son (2013), Northern Hemisphere blocking frequency and duration in the CMIP5 models, *J. Geophys. Res. Atmos.*, *118*, 1179–1188, doi:10.1002/jgrd.50143.

Francis, J. A., and S. J. Vavrus (2012), Evidence linking Arctic amplification to extreme weather in mid-latitudes, *Geophys. Res. Lett.*, *39*, L06801, doi:10.1029/2012GL051000.

Harvey, B., L. Shaffrey, and T. Woollings (2013), Equator-to-pole temperature differences and the extra-tropical storm track responses of the CMIP5 climate models, *Clim. Dyn.*, *43*(5–6), 1171–1182, doi:10.1007/s00382-013-1883-9.

Harvey, B. J., L. C. Shaffrey, and T. J. Woollings (2015), Deconstructing the climate change response of Northern Hemisphere winter storm tracks, *Clim. Dyn.*, *45*, 2847–2860, doi:10.1007/s00382-015-2510-8.

Hassanzadeh, P., and Z. Kuang (2015), Blocking variability: Arctic Amplification versus Arctic Oscillation, *Geophys. Res. Lett.*, *42*, 8586–8595, doi:10.1002/2015GL065923.
Hassanzadeh, P., Z. Kuang, and B. F. Farrell (2014), Responses of midlatitude blocks and wave amplitude changes in the meridional temperature gradient in an idealized dry GCM, *Geophys. Res. Lett.*, *41*, 5223–5232, doi:10.1002/2014GL060674.
Held, I. M. (1993), Large-scale dynamics and global warming, *Bull. Am. Meteorol. Soc.*, *74*(2), 228–241.
Holmes, C. R., T. Woollings, E. Hawkins, and H. de Vries (2015), Robust future changes in temperature variability under greenhouse gas forcing and the relationship with thermal advection, *J. Clim.*, *29*, 2221–2236, doi:10.1175/JCLI-D-14-00735.1.
Johns, T. C., et al. (2006), The new Hadley Centre climate model (HadGEM1): Evaluation of coupled simulations, *J. Clim.*, *19*, 1327–135, doi:10.1175/JCLI3712.1.
Liu, J., J. A. Curry, H. Wang, M. Song, and R. M. Horton (2012), Impact of declining Arctic sea ice on winter snowfall, *Proc. Natl. Acad. Sci. U. S. A.*, *109*(11), 4074–4079.
Magnusdottir, G., C. Deser, and R. Saravanan (2004), The effects of North Atlantic SST and sea ice anomalies on the winter circulation in CCM3. Part I: Main features and storm track characteristics of the response, *J. Clim.*, *17*, 857–876, doi:10.1175/1520-0442(2004)017<0857:TEONAS>2.0.CO;2.
Martin, G. M., M. A. Ringer, V. D. Pope, A. Jones, C. Dearden, and T. J. Hinton (2006), The physical properties of the atmosphere in the new Hadley Centre Global Environmental Model (HadGEM1). Part I: Model description and global climatology, *J. Clim.*, *19*, 1274–1301, doi:10.1175/JCLI3636.1.
Masato, G., B. J. Hoskins, and T. Woollings (2013), Winter and summer Northern Hemisphere blocking in CMIP5 models, *J. Clim.*, *26*, 7044–7059, doi:10.1175/JCLI-D-12-00466.1.
Masato, G., T. Woollings, and B. J. Hoskins (2014), Structure and impact of atmospheric blocking over the Euro-Atlantic region in present-day and future simulations, *Geophys. Res. Lett.*, *41*, 1051–1058, doi:10.1002/2013GL058570.
Matsueda, M. (2009), Blocking predictability in operational medium-range ensemble forecasts, *SOLA*, *5*, 113–116, doi:10.2151/sola.2009-029.
Matsueda, M. (2010), Predictability of Euro-Russian blocking in summer of 2010, *Geophys. Res. Lett.*, *38*, L06801, doi:10.1029/2010GL046557.
Matsueda, M., R. Mizuta, and S. Kusunoki (2009), Future change in wintertime atmospheric blocking simulated using a 20-km-mesh atmospheric global circulation model, *J. Geophys. Res.*, *114*, D12114, doi:10.1029/2009JD011919.
Mori, M., M. Watanabe, H. Shiogama, J. Inoue, and M. Kimoto (2014), Robust Arctic sea-ice influence on the frequent Eurasian cold winters in past decades, *Nat. Geosci.*, *7*, 869–873, doi:10.1038/ngeo2277.
Pelly, J. L., and B. J. Hoskins (2003), A new perspective on blocking, *J. Atmos. Sci.*, *60*, 743–755, doi:10.1175/1520-0469(2003)060<0743:ANPOB>2.0.CO;2.
Pfahl, S., and H. Wernli (2012), Quantifying the relevance of atmospheric blocking for co-located temperature extremes in the Northern Hemisphere on (sub-)daily time scales, *Geophys. Res. Lett.*, *39*, L12807, doi:10.1029/2012GL052261.
Rex, D. F. (1950), Blocking action in the middle troposphere and its effect upon regional climate, *Tellus*, *2*, 196–211, doi:10.1111/j.2153-3490.1950.tb00331.x.
Scaife, A. A., T. Woollings, J. Knight, G. Martin, and T. Hinton (2010), Atmospheric blocking and mean biases in climate models, *J. Clim.*, *23*, 6143–6152, doi:10.1175/2010JCLI3728.1.
Scherrer, S. C., M. Croci-Maspoli, C. Schwierz, and C. Appenzeller (2005), Two-dimensional indices of atmospheric blocking and their statistical relationship with winter climate patterns in the Euro-Atlantic region, *Int. J. Climatol.*, *26*, 233–249, doi:10.1002/joc.1250.
Shepherd, T. G. (2015), Atmospheric circulation as a source of uncertainty in climate change projections, *Nat. Geosci.*, *7*, 703–708, doi:10.1038/ngeo2253.
Sillmann, J., and M. Croci-Maspoli (2009), Euro-Atlantic blocking and extreme events in present and future climate simulations, *Geophys. Res. Lett.*, *36*, L10702, doi:10.1029/2009GL038249.
Tibaldi, S., and F. Molteni (1990), On the operational predictability of blocking, *Tellus A*, *42*, 343–365.
Torn, R. D., J. S. Whitaker, P. Pegion, T. M. Hamill, and G. J. Hakim (2012), Diagnosis of the source of GFS medium-range track errors in Hurricane Sandy (2012), *Mon. Weather Rev.*, *143*, 132–152, doi:10.1175/MWR-D-14-00086.
Wilson, C., B. Sinha, and R. G. Williams (2009), The effect of ocean dynamics and orography on atmospheric storm tracks, *J. Clim.*, *22*, 3689–3702, doi:10.1175/2009JCLI2651.1.
Woollings, T. (2010), Dynamical influences on European climate: An uncertain future, *Philos. Trans. R. Soc. A*, *368*, 3733–3756, doi:10.1098/rsta.2010.0040.
Woollings, T., B. Hoskins, M. Blackburn, and P. Berrisford (2008), A new Rossby wave-breaking interpretation of the North Atlantic Oscillation, *J. Atmos. Sci.*, *65*, 609–626, doi:10.1175/2007JAS2347.1.
Woollings, T., B. Harvey, and G. Masato (2015), Arctic warming, atmospheric blocking and cold European winters in CMIP5 models, *Environ. Res. Lett.*, *9*, 014002, doi:10.1088/1748-9326/9/1/014002.